

## Two-band luminescence from an intrinsic defect in spherical and terraced MgO nanoparticles

Peter V. Pikhitsa, Changhyuk Kim, Sukbyung Chae, Seungha Shin, Sekwon Jung, Mamoru Kitaura, Shin-ichi Kimura, Kazutoshi Fukui, and Mansoo Choi

Citation: *Applied Physics Letters* **106**, 183106 (2015); doi: 10.1063/1.4918804

View online: <http://dx.doi.org/10.1063/1.4918804>

View Table of Contents: <http://scitation.aip.org/content/aip/journal/apl/106/18?ver=pdfcov>

Published by the [AIP Publishing](#)

---

### Articles you may be interested in

[On the role of Fe ions on magnetic properties of doped TiO<sub>2</sub> nanoparticles](#)

*Appl. Phys. Lett.* **106**, 142404 (2015); 10.1063/1.4917037

[Defect structure of ultrafine MgB<sub>2</sub> nanoparticles](#)

*Appl. Phys. Lett.* **105**, 202605 (2014); 10.1063/1.4902375

[Influence of defect states on the secondary electron emission yield  \$\gamma\$  from MgO surface](#)

*J. Appl. Phys.* **95**, 8419 (2004); 10.1063/1.1751239

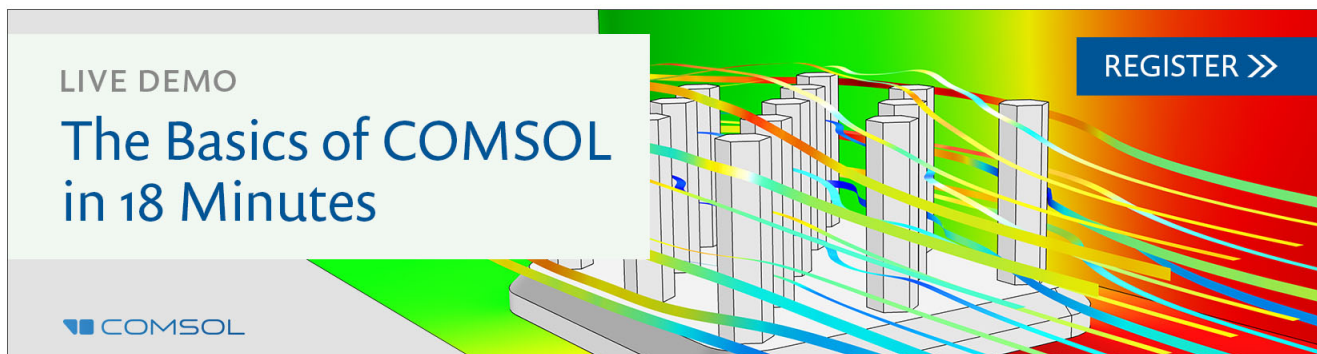
[On the accurate prediction of the optical absorption energy of F-centers in MgO from explicitly correlated ab initio cluster model calculations](#)

*J. Chem. Phys.* **115**, 1435 (2001); 10.1063/1.1381011

[Optical properties of surface and bulk F centers in MgO from ab initio cluster model calculations](#)

*J. Chem. Phys.* **108**, 7835 (1998); 10.1063/1.476220

---

The advertisement features a 3D bar chart with several vertical bars of varying heights. Overlaid on the chart are several colorful, flowing lines in shades of blue, green, yellow, and red, suggesting data analysis or simulation results. The background is a gradient from green to red. In the top left, the text 'LIVE DEMO' is in a light blue box. Below it, 'The Basics of COMSOL in 18 Minutes' is written in a large, bold, blue font. In the bottom left, the COMSOL logo is visible. In the top right, a dark blue button with white text says 'REGISTER >>'.

LIVE DEMO

# The Basics of COMSOL in 18 Minutes

COMSOL

REGISTER >>

## Two-band luminescence from an intrinsic defect in spherical and terraced MgO nanoparticles

Peter V. Pikhitsa,<sup>1,a),b)</sup> Changhyuk Kim,<sup>1,b)</sup> Sukbyung Chae,<sup>1</sup> Seungha Shin,<sup>1</sup> Sekwon Jung,<sup>1</sup> Mamoru Kitaura,<sup>2</sup> Shin-ichi Kimura,<sup>3</sup> Kazutoshi Fukui,<sup>4</sup> and Mansoo Choi<sup>1,a)</sup>

<sup>1</sup>Global Frontier Center for Multiscale Energy Systems, Division of WCU Multiscale Mechanical Design, School of Mechanical and Aerospace Engineering, Seoul National University, Seoul 151-744, South Korea

<sup>2</sup>Department of Physics, Faculty of Science, Yamagata University, Kojirakawa 1-4-12, Yamagata 990-8560, Japan

<sup>3</sup>UVSOR Facility, Institute for Molecular Science and the Graduate University for Advanced Studies, Okazaki 444-8585, Japan

<sup>4</sup>Department of Electrical and Electronics Engineering, Faculty of Engineering, University of Fukui, Fukui 910-8507, Japan

(Received 28 January 2015; accepted 10 April 2015; published online 5 May 2015)

Luminescent defect centers in wide bandgap materials such as MgO are of great interest for science and technology. Magnesium oxide nanocubes obtained by the self-combustion of Mg metal have long exhibited only a broad 2.9 eV cathodoluminescence band owing to oxygen vacancies ( $F$  centers). However, in this work, a room-temperature ultraviolet 4.8 eV cathodoluminescence band has been observed coincident with a 2.5 eV band of the same intensity from an unexplored intrinsic defect in MgO terraced nanocubes and nanospheres produced from Mg metal combustion in an  $H_2/O_2$  flame. Synchrotron radiation excitation spectra reveal that the excitation energy at the onset of both bands is just above the bandgap energy of 7.7 eV, where electrons and holes are generated. We determine that a defect, responsible for both emission bands, creates proximal anion-cation vacancy pairs named  $P$  centers that may appear instead of  $F$  centers because of changes in the MgO nanoparticle growth conditions. © 2015 AIP Publishing LLC.

[<http://dx.doi.org/10.1063/1.4918804>]

It has long been known that defects determine the optical properties of bandgap crystalline materials interesting for applications. Wide bandgap rock salt cubic crystals such as NaCl and MgO are perfect platforms to study Schottky defects, which are anion (cation) vacancies called  $F$  ( $V$ ) centers possessing various charge states with trapped electrons (holes). In monovalent alkali halides, the color centers and the pairs of vacancies are understood well enough that the  $F$  centers are being used for lasing.<sup>1</sup> However, in divalent MgO, there is still a controversy about these defects concerning the position of their energy states within the bandgap and their interaction with the excitation.<sup>2-5</sup> Recent calculations<sup>6</sup> have provided a description of  $F$  centers in MgO that agree perfectly with the experimental absorption measurements of  $F^+$  and  $F^0$  charge states. Much less is known about the close pairs of anion-cation vacancies when the entire MgO molecule is absent from the lattice (so-called  $P$  center<sup>3</sup>), although *ab initio* calculations have shown that, among complex Schottky and Frenkel defects, the  $P^-$  center possesses the lowest formation energy.<sup>3,7</sup> Its electronic state has also been calculated<sup>3,8</sup> and an attempt to experimentally observe this and other color centers on the surface of MgO has been made.<sup>9</sup>

The bulk MgO  $F$  centers are active in cathodoluminescence (CL) with the characteristic broad emission bands of  $F^0$  ( $\sim 520$  nm) and  $F^+$  ( $\sim 390$  nm). Ultraviolet (UV) CL has

been also observed, though mostly at low temperatures, induced by aliovalent impurities such as  $Al^{3+}$  and  $Si^{4+}$  where all of the UV bands are strictly above 5 eV.<sup>10,11</sup> At the same time, aliovalent impurities are known to suppress the creation of  $F$  centers so that these observed UV impurity bands are followed by suppressed  $F$  center bands. At an even lower UV energy of 4.8 eV, the CL that has been claimed as originating from  $V^-$  centers has been observed in electron/X-ray-irradiated MgO<sup>2,12,13</sup> but has remained elusive. The difficulty has been that only a single broad and featureless UV band is typically observed, so the observation of more bands originating from the same defect would be of great use, whereupon the UV band at 4.8 eV would find its place in the line graph of Fig. 5 from Ref. 11 that contains the energies of trapping hole centers, such as  $V_{Al}$ ,  $[Li]^0$ , and  $[Be]^+$ , becoming the ending point of the line with presumably the highest thermal decay temperature that exceeds 500 K. Note that a previous study<sup>14</sup> has reported 4.8 eV UV CL accompanied by 2.5 eV CL from pure MgO nanoparticles, which were intended to be applied in fluorescence enhancement layers in liquid crystal displays, although the origin and physics of the CL spectra were not discussed therein.

Here, we report two-band room-temperature CL and low-temperature synchrotron radiation (SR) spectra from MgO nanoparticles, prepared in an  $H_2/O_2$  flame or under  $CO_2$  laser irradiation, and discuss the possible origin of the two bands. Both bands are found to arise in the SR spectra simultaneously when the excitation energy exceeds 7.7 eV of the bandgap. We attribute the room-temperature UV

<sup>a)</sup>Authors to whom correspondence should be addressed. Electronic addresses: peter@snu.ac.kr and mchoi@snu.ac.kr.

<sup>b)</sup>P. V. Pikhitsa and C. Kim contributed equally to this work.

(260 nm: 4.8 eV) CL band along with the concurrent 2.5 eV emission band (Fig. 1(c)) to a robust bandgap defect, which is presumably the  $P^-$  center. We find that Mg-metal combustion that is modified either by an oxy-hydrogen flame<sup>15</sup> (Fig. 1(a)) or by a 10.56  $\mu\text{m}$  continuous wave (cw) CO<sub>2</sub> laser (Fig. 1(b)) creates terraced and spherical MgO nanoparticles (UV-MgO) that contain the defect responsible for both bands but which are devoid of  $F^+$  centers. On the contrary, MgO nanoparticles generated in Mg-metal combustion (in a dry gas atmosphere)<sup>16</sup> or under insufficient modification of the combustion process by an H<sub>2</sub>/O<sub>2</sub> flame or CO<sub>2</sub> laser irradiation, exhibit only  $F^+$  ( $\sim 420$  nm: 2.9 eV) CL (Fig. 1(d)) or a SR band instead of the two-band CL/SR (non-UV-MgO). Therefore, we link the pronounced nanoparticle morphology change to the change of the defect that, in turn, is responsible for the luminescence.

Let us show that both bands have the common origin of a bulk intrinsic defect. To exclude any participation of extrinsic defects, the possible effect of an impurity upon the two-band emission has been thoroughly examined, because UV CL strictly above 5 eV has been previously found for Al-, Be-, or Si-doped MgO crystals or powders.<sup>10,11</sup> No correlation can be found between the existence either of the two-band CL or the  $F^+$  (2.9 eV) CL and the impurity levels (supplementary material,<sup>17</sup> Table SI) in our samples, and the X-ray diffraction (XRD) spectra also confirm the perfect cubic structure of the nanoparticles (Fig. S1). There is the separate question of the role of hydrogen and hydroxyls in the luminescence for the UV-MgO nanoparticles produced inside the H<sub>2</sub>/O<sub>2</sub> flame. Although we successfully generate UV-MgO nanoparticles without an H<sub>2</sub>/O<sub>2</sub> flame by modifying the Mg metal combustion in dry air or oxygen using a cw CO<sub>2</sub> laser, a previous study has demonstrated that an additional weak 2.9 eV band may arise from hydrogen at

low-coordination (LC) sites of 3–10 nm MgO cubes.<sup>18</sup> Additionally, Fourier transform infrared (FT-IR) vibrational spectroscopy shows the presence of an OH vibrational band located around 3500  $\text{cm}^{-1}$  (Fig. S2). However, this weak band is quite similar for both UV and non-UV-MgO nanoparticles and is an unlikely cause for the dramatic difference in the CL spectra. To prove conclusively that hydroxyls or surface defects play no role in producing these bands, we soak the samples in water for several hours along with sonication whereupon, in spite of a considerable reshaping of the MgO nanoparticles, the results confirm that there is no change in the shape of CL spectra for both the UV and non-UV CL (Fig. S3). Some reduction in the CL intensity arises from the appearance of hexagonal Mg(OH)<sub>2</sub> (brucite) that is clearly seen from XRD data as well as from transmission electron microscopy (TEM) images of the water-etched nanoparticles (Fig. S4). Therefore, neither the presence of hydrogen nor hydroxyls nor the dramatic reconstruction of the surface and its subsequent defects can modify or destroy the robust bulk defects responsible for the UV CL from UV-MgO.

Room-temperature CL spectra at 3–30 keV acceleration voltages from a scanning electron microscope (SEM-CL) (Gatan MonoCL3, Japan) are given in Figs. 1(c), 1(d), and 2. The UV-MgO obtained from the oxy-hydrogen diffusion flame or from CO<sub>2</sub> laser irradiation exhibit a 4.8 eV UV band and a 2.5 eV band in CL (Fig. 1(c)), together with several other distinct bands located at 7.7 eV arising from band-to-band transitions (Fig. S5) and at 1.65 eV arising from Mn impurities (Figs. 1 and 2). The MgO cubes (inset in Fig. 1(d)) obtained from self-burning in air, however, do not exhibit the two 4.8 and 2.5 eV bands, but instead exhibit a 2.9 eV band from the  $F^+$  center with the Mn impurity band of 1.65 eV (Fig. 1(d)). For the smallest 5 nm-diameter

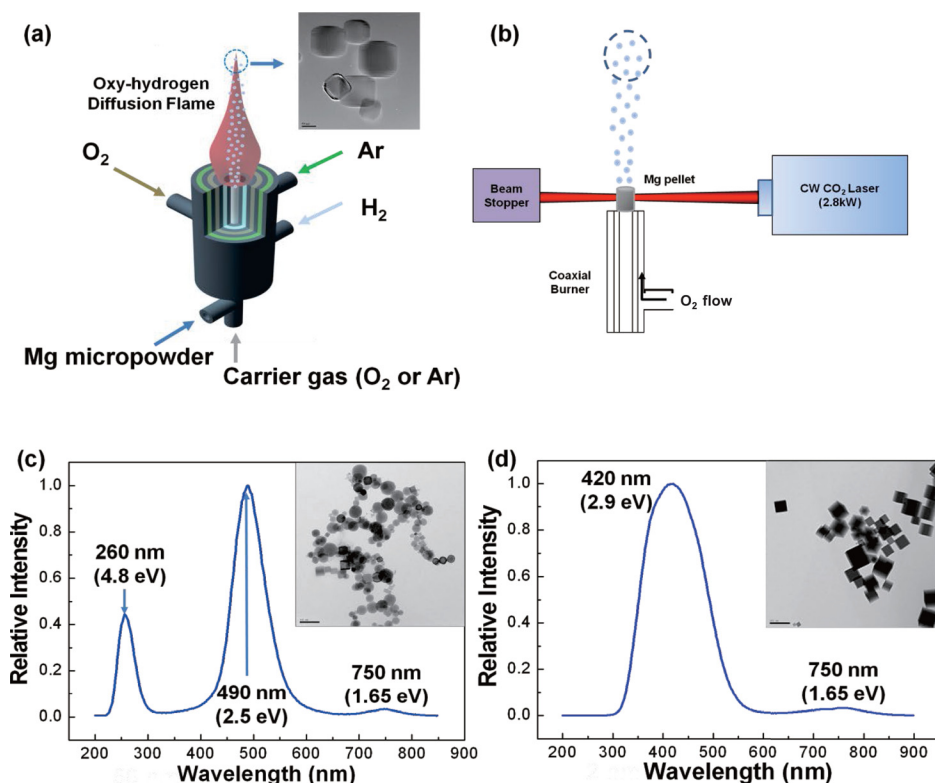


FIG. 1. MgO nanoparticles obtained in Mg combustion in an H<sub>2</sub>/O<sub>2</sub> flame or under CO<sub>2</sub> laser irradiation and the CL emanating from them. Schematic of a section of the experimental set-up with (a) the oxy-hydrogen flame (inset shows a TEM image of terraced nanoparticles) or (b) a continuous wave CO<sub>2</sub> laser. (c) Two-band CL from spherical MgO nanoparticles (inset) obtained with oxy-hydrogen flame. (d) The CL from MgO nanocubes (inset) obtained by Mg combustion in air. (Insets) Transmission electron microscope images of the samples. Scale bars represent (a) 50 nm, (c) 100 nm, and (d) 200 nm.

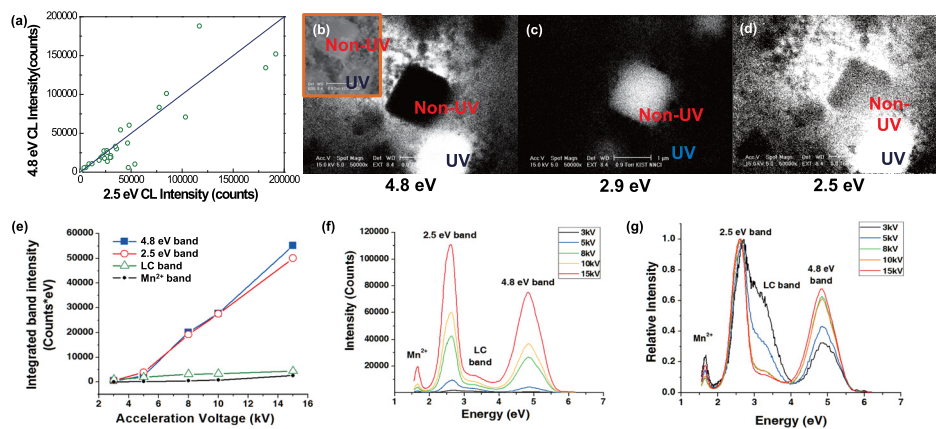


FIG. 2. Intensity, spatial and depth-dependent correlations of the CL from MgO nanoparticles. (a) Correlation between the integrated intensities of the 4.8 and 2.5 eV CL bands. The straight line shows the direct proportionality law. (b) CL spot image at 4.8 eV. (Inset) Scanning electron microscope image of the same spot. (c) CL spot image at 2.9 eV. (d) CL spot image at 2.5 eV. (b) and (d) show good coincidence. (e)–(g) An acceleration voltage sweep from 3 to 15 kV supports the correlation (the intensities of 4.8 and 2.5 eV bands approach 1:1 ratio at voltages  $>5$  kV) and bulk nature (the intensities dominating at voltages  $>5$  kV) of the two-band CL when compared with the tendency of the LC surface defect band to decrease in proportion. (g) Normalized spectra of (f) based upon the peak intensity of the 2.5 eV band. Notice that only at the lowest acceleration voltages of 3 and 5 keV, which mostly excite the near-surface and surface defects, the LC band increases at the cost of the 4.8 eV UV band, thus slightly violating the law of proportionality between the 4.8 and 2.5 eV bands.

nanoparticles separated by centrifugation and sedimentation, additional bands can be seen at around 3.2–3.3 eV (Figs. 2(f) and 2(g)), which come from abundant LC oxygen defect centers (e.g., corners of terraces and cubes)<sup>19</sup> together with enhanced Mn impurity peaks. The increase of the LC band in the smaller nanoparticles demonstrates that it is a surface CL band. Meanwhile, the other bands remain unaltered because they are bulk in origin, excepting the  $\text{Mn}^{2+}$  band, which may indicate that the impurities tend to come to the surface. Importantly, a strong correlation between the 2.5 and 4.8 eV bands from UV-MgO is observed for all samples obtained with different carrier gases ( $\text{O}_2$  or Ar) and for different CL spot positions (Fig. 2(a)), which indicates that the two CL bands originate from the same defect.

Spatially resolved CL supports the division of the MgO nanoparticles into two types. The UV-emitting nanoparticles exclusively show both 4.8 and 2.5 eV bands, where the band intensities at 4.8 and 2.5 eV from different UV nanoparticles statistically follow the proportionality law  $I(4.8 \text{ eV}) = I(2.5 \text{ eV})$ , as shown in Fig. 2(a). On the other hand, individual non-UV nanoparticles show only the  $F^+$  (2.9 eV) band. Spatially resolved CL images in Figs. 2(b)–2(d) and S6(a)–S6(c) clearly show a perfect spatial correlation of the 4.8 and 2.5 eV bands. Indeed, the spot image in Fig. 2(b) and the area image in Fig. S6(a) for the UV band show an overlap with the corresponding images for 2.5 eV in Figs. 2(d) and S6(c), while the images for 2.9 eV do not overlap with either the UV or 2.5 eV emitting sites. These observations provide proof that the two-band CL comes from a specific type of nanoparticle that can be created only under combustion in an  $\text{H}_2/\text{O}_2$  flame or under  $\text{CO}_2$  laser irradiation.

The SEM-CL acceleration voltage is swept from 3–15 kV to vary the penetration depth of the electron beam from tens of nm to a  $\mu\text{m}$ , and the correlation between the two CL bands is found to be preserved, while the band intensities increase with the penetration depth (Figs. 2(e) and 2(f)). At small penetration depths and at low voltages, the surface LC defect contribution is comparable to the two-

band CL (Fig. 2(e) and the normalized spectra in Fig. 2(g) with the somewhat reduced 4.8 eV band); but at higher voltages ( $>5$  kV) with penetration into the bulk, the two correlated CL bands dominate and their ratio comes to 1:1 as dictated by the correlation law that we established (Figs. 2(e) and 2(g)). Meanwhile, the LC defect band, which is a surface defect band, grows much more slowly with the increase of the acceleration voltage and penetration depth, thereby proving that the two-band CL originate from centers in the bulk and that the surface defects can be rejected as a possible cause of the two-band CL.

The most clarifying experiment to confirm the common origin of the two bands and to determine why the electron beam in CL is so efficient for their excitation is accomplished by measuring the photoluminescence (PL) under SR, carried out at the visible–vacuum UV (VIS-VUV) luminescence beamline BL3B of UVSOR-III in Japan. Figure 3 compares the PL spectra, taken at 8 K, for photon excitation energies swept through the forbidden band and up to 10 eV from the UV-MgO (Fig. 3(a)) and the non-UV-MgO cubes (Fig. 3(b)). It is clear that the two PL bands observed in CL arise simultaneously at 7.7 eV and persist as the excitation energy sweeps deeper into the conduction band (Fig. 3(a)). This is a strong indication that both bands (marked by red circles in Fig. 3(a)) have the same origin and that electrons and holes from the conduction band are solely responsible and necessary for the excitation of the two bands, similar to the electron and hole “shower” in CL, when it is understood that a photon of 8 eV leads to the formation in MgO of a conduction electron and a hole that do not undergo transformation into a self-trapped state. Nothing comparable happens in the non-UV-MgO cubes devoid of the defect needed for the two band PL excitation (Fig. 3(b)), wherein only an intra-center excitation at  $\sim 6$  eV manifests itself in a 420 nm emission band. The SR experiment can be compared with that performed on doped and undoped MgO nanoparticles<sup>20</sup> where, although 212 and 235 nm emission bands have always been observed from doped MgO nanoparticles, no concurrent 490 nm band has been excited above 7.7 eV,

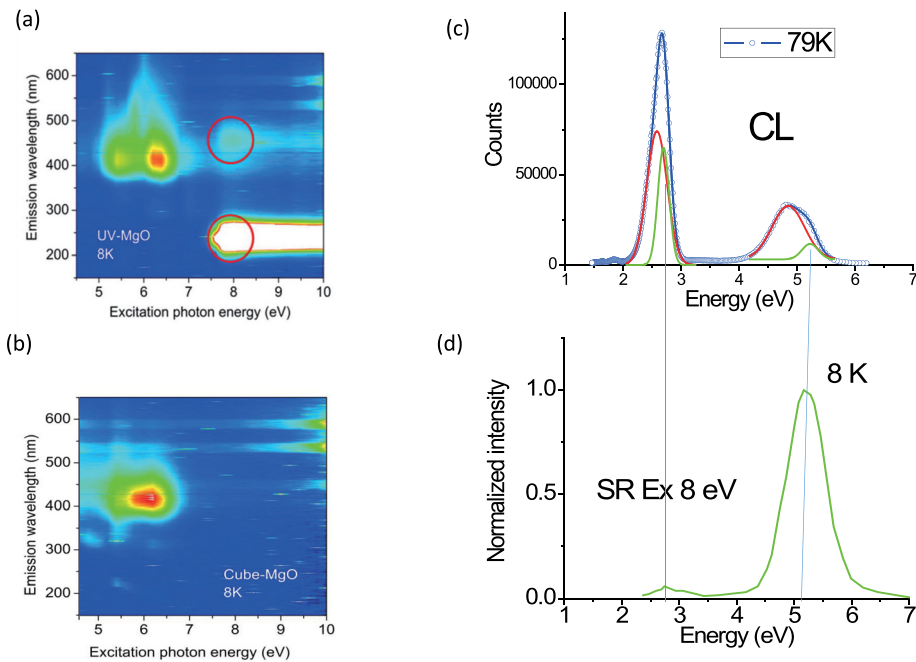


FIG. 3. Photoluminescence spectra vs. excitation energy from synchrotron radiation (intensity grows from blue to red). (a) Red circles marking correlated emission bands at 4.8 eV (upper) and 2.5 eV (lower) from UV-emitting MgO. The  $F^+$  band at 420 nm is from the non-UV-MgO present in the powder sample. (b) Emission from non-UV-MgO cubes, where the  $F^+$  band at 420 nm is present but the 4.8 and 2.5 eV bands are absent. (c) CL spectrum for UV-MgO taken at 79 K (blue) and the deconvoluted spectral peaks (red and green curves). The additional two-band spectrum (green curve) is compared with (d) the two-band synchrotron radiation spectrum (not corrected for intensity magnitude) excited at 8 eV and 8 K taken from (a).

which indicates the similar but different nature of the defect responsible for the two-band luminescence that is reported here. At the same time, a  $\sim 400$  nm band has been observed<sup>20</sup> but only with a sub-band excitation, as we also observe for MgO cubes. This certainly indicates that our cubic non-UV-MgO nanoparticles behave like undoped MgO crystals.<sup>20</sup> Meanwhile, our spherical and terraced nanoparticles exhibit the two bands above 7.7 eV, manifesting the excitation of some peculiar defect by the separate electrons and holes. The phenomenon closely resembles KI crystals where the irradiation of the crystal by 7.7 or 13 eV photons, which create separate electrons and holes, causes the appearance of two emission bands at 4.15 and 3.31 eV.<sup>21</sup> These singlet and triplet components of the self-trapped exciton emission arise owing to the recombination of electrons with relaxed self-trapped holes. Excitations lower than the bandgap width produce only a single band.<sup>21</sup>

The  $P^-$  center concept may account for the 4.8 and 2.5 eV two-band CL/SR and explain why it has not previously been detected in spite of considerable efforts to find a UV CL from pure MgO.<sup>21,22</sup> The two-band emission may be viewed in this way: instead of any aliovalent charge-compensating substitution impurity, the  $V^{--}$  center neighbors with the  $F^+$  center (thus constituting the  $P^-$  center) and emits the lowest energy of 4.8 eV, ending up the line of emission band energies.<sup>11</sup> Meanwhile, the presence of the attached  $F^+$  center, screened by the nearby  $V^{--}$  center, reveals itself in the 2.5 eV concurrent emission with a wavelength of 490 nm, similar to 520 nm of the neutral  $F^0$  center in bulk MgO. However, to create the MgO  $P^-$  center di-vacancy (which is a threshold phenomenon<sup>3</sup>) it is necessary to generate the MgO using an extreme method which can produce defects quite different from the  $F$  centers that result from self-combustion in dry air.

The discovery of two-band room-temperature CL from spherical and terraced MgO nanoparticles may find applications in defect-center lasers based upon MgO and in spectral transformers.<sup>21</sup> The two-band CL may also have applications

in the geosciences because its presence or absence should be useful to distinguish the history of MgO formation in the Earth's mantle or in planetary nebula.

This work was accomplished with financial support from the Global Frontier Center for Multiscale Energy Systems (2011-0031561) supported by the Korean Ministry of Science and Technology. We thank Daegy Kim for assistance with the CO<sub>2</sub> laser experiment. Financial support from the BK21 program and WCU (World Class University) multiscale mechanical design program (R31-2008-000-10083-0) through the Korea Research Foundation is gratefully acknowledged. A part of this work was supported by the use-of-UVSOR Facility Program (BL3B, Proposal No. 25-T502) of the Institute for Molecular Science.

<sup>1</sup>B. Henderson and G. F. Imbusch, *Optical Spectroscopy of Inorganic Solids* (Oxford University Press, USA, 2006), Vol. 44.

<sup>2</sup>R. T. Williams, J. W. Williams, T. J. Turner, and K. H. Lee, *Phys. Rev. B* **20**, 1687 (1979).

<sup>3</sup>A. Gibson, R. Haydock, and J. P. LaFemina, *Phys. Rev. B* **50**, 2582 (1994).

<sup>4</sup>G. H. Rosenblatt, M. W. Rowe, G. P. Williams, R. T. Williams, and Y. Chen, *Phys. Rev. B* **39**, 10309 (1989).

<sup>5</sup>G. P. Summers, T. M. Wilson, B. T. Jeffries, H. T. Tohver, Y. Chen, and M. M. Abraham, *Phys. Rev. B* **27**, 1283 (1983).

<sup>6</sup>P. Rinke, A. Schleife, E. Kioupakis, A. Janotti, C. Rödl, F. Bechstedt, M. Scheffler, and C. G. Van de Walle, *Phys. Rev. Lett.* **108**, 126404 (2012).

<sup>7</sup>C. A. Gilbert, S. D. Kenny, R. Smith, and E. Sanville, *Phys. Rev. B* **76**, 184103 (2007).

<sup>8</sup>L. Ojamäe and C. Pisani, *J. Chem. Phys.* **109**, 10984 (1998).

<sup>9</sup>T. König, G. H. Simon, H.-P. Rust, G. Pacchioni, M. Heyde, and H.-J. Freund, *J. Am. Chem. Soc.* **131**, 17544 (2009).

<sup>10</sup>K. A. Kalder, T. N. Kyarner, C. B. Lushchik, A. F. Malysheva, and R. V. Milenina, *Zh. Prikl. Spektrosk.* **25**, 1250 (1976).

<sup>11</sup>S. A. Dolgov, T. Karner, A. Lushchik, A. Maaros, S. Nakonechnyi, and E. Shablonin, *Phys. Solid State* **53**, 1244 (2011).

<sup>12</sup>K. J. Caulfield, R. Cooper, and J. F. Boas, *J. Chem. Phys.* **92**, 6441 (1990).

<sup>13</sup>S. Benedetti, H. M. Benia, N. Nilius, S. Valeri, and H. J. Freund, *Chem. Phys. Lett.* **430**, 330 (2006).

<sup>14</sup>Y.-K. Lee, S.-T. Heo, Y.-K. Lee, and D.-G. Lee, *Trans. Electr. Electron. Mater.* **11**, 186 (2010).

- <sup>15</sup>S. Yang, Y. H. Jang, C. H. Kim, C. Hwang, J. Lee, S. Chae, S. Jung, and M. Choi, *Powder Technol.* **197**, 170 (2010).
- <sup>16</sup>I. S. Altman, P. V. Pikhitsa, and M. Choi, in *Gas Phase Nanoparticle Synthesis*, edited by C. Granqvist, L. Kish, and W. Marlow (Kluwer Academic Publishers, Dordrecht, London, Boston, 2004), pp. 43–67.
- <sup>17</sup>See supplementary material at <http://dx.doi.org/10.1063/1.4918804> for an additional table and figures.
- <sup>18</sup>M. Müller, S. Stankic, O. Diwald, E. Knözinger, P. V. Sushko, P. E. Trevisanutto, and A. L. Shluger, *J. Am. Chem. Soc.* **129**, 12491 (2007).
- <sup>19</sup>S. Stankic, M. Müller, O. Diwald, M. Sterrer, E. Knözinger, and J. Bernardi, *Angew. Chem., Int. Ed.* **44**, 4917 (2005).
- <sup>20</sup>W.-J. Kuang, Q. Li, Y.-X. Chen, K. Hu, N.-H. Wang, F.-L. Xing, Q. Yan, S.-S. Sun, Y. Huang, Y. Tao *et al.*, *J. Phys. D: Appl. Phys.* **46**, 365501 (2013).
- <sup>21</sup>A. Lushchik, E. Feldbach, R. Kink, Ch. Lushchik, M. Kirm, and I. Martinson, *Phys. Rev. B* **53**, 5379 (1996).
- <sup>22</sup>A. Lushchik, C. Lushchik, A. Kotlov, I. Kudryavtseva, A. Maaros, V. Nagirnyi, and E. Vasil'chenko, *Radiat. Meas.* **38**, 747 (2004).